Sensors & Transducers, Vol. 193, Issue 10, October 2015, pp. 23-32

Sensors & Transducers

http://www.sensorsportal.com

Novel Smart Glove Technology as a Biomechanical Monitoring Tool

[1] Brendan O'FLYNN, [1] J. T. SANCHEZ, [1] S. TEDESCO, [2] B. DOWNES, [3] J. CONNOLLY, [3] J. CONDELL, [3] K. CURRAN

[1] Tyndall National Institute, University College Cork, Cork, Ireland
[2] Waterford Institute of Technology, Waterford, Ireland
[3] Computing & Engineering, Magee College, Ulster University, Derry, N. Ireland
[1] Tel.: +353 21 2346041, fax: +353 21 49004958
E-mail: brendan.oflynn@tyndall.ie

Received: 31 August 2015 /Accepted: 5 October 2015 /Published: 30 October 2015

Abstract: Developments in Virtual Reality (VR) technology and its overall market have been occurring since the 1960s when Ivan Sutherland created the world's first tracked head-mounted display (HMD) – a goggle type head gear. In society today, consumers are expecting a more immersive experience and associated tools to bridge the cyber-physical divide. This paper presents the development of a next generation smart glove microsystem to facilitate Human Computer Interaction through the integration of sensors, processors and wireless technology. The objective of the glove is to measure the range of hand joint movements, in real time and empirically in a quantitative manner. This includes accurate measurement of flexion, extension, adduction and abduction of the metacarpophalangeal (MCP), Proximal interphalangeal (PIP) and Distal interphalangeal (DIP) joints of the fingers and thumb in degrees, together with thumb-index web space movement. This system enables full real-time monitoring of complex hand movements. Commercially available gloves are not fitted with sufficient sensors for full data capture, and require calibration for each glove wearer. Unlike these current state-of-the-art data gloves, the UU / Tyndall Inertial Measurement Unit (IMU) glove uses a combination of novel stretchable substrate material and 9 degree of freedom (DOF) inertial sensors in conjunction with complex data analytics to detect joint movement. Our novel IMU data glove requires minimal calibration and is therefore particularly suited to multiple application domains such as Human Computer interfacing, Virtual reality, the healthcare environment. *Copyright © 2015 IFSA Publishing, S. L.*

Keywords: Data glove, IMU, Virtual reality, Arthritis, Joint Stiffness, Hand Monitoring.

1. Introduction

Data gloves contain strategically placed sensors controlled by circuitry that communicates finger joint movement to an end device. In recent years data gloves have been evaluated by researchers as an effective replacement for the universal goniometer (UG) [12–17]. Results showed comparable repeatability to the UG with the added advantage of simultaneous angular measurement and removal of intra-tester and inter-tester reliability problems associated with the UG. Data gloves however have several drawbacks; they require laborious calibration, are difficult to don and doff; and are designed to fit specific hand sizes and so require small, medium and large gloves to fit all hand variations. The first

iteration of our system was developed using a state-of-the-art 5DT Ultra 14 data glove [18]. In this paper, our inertial measurement unit (IMU) Smart Glove is evaluated against this data glove for accuracy and repeatability and further validated using the Vicon motion capture system [19].

Virtual reality (VR) systems can be segmented into one of three experiences: non-immersive, semi-immersive, and fully immersive. Non-immersive systems would be those that can be visualized on a desktop computer. Semi-immersive VR environments incorporate images projected on the walls (e.g., cave automatic virtual environment, better known by the acronym CAVE). For a period of time, the user may superficially succumb to the perception of "being there", but all the while still be aware of their real world surroundings. Finally, there is fully-immersive technology. In these systems, real-world visual and auditory cues are completely blocked out and the user has a sensory experience of being inside the computer-generated world. The experience is made ever more real through the use of hand-held and/or wearable devices that in some cases deliver haptic feedback which invoke sensations of touch. To enable Human Computer Interaction (HCI) in this immersive fashion, high precision data acquisition systems need to be developed which are accurate, require minimal calibration and which provide real-time data streams wirelessly. The development of such a glove based system lends itself to multiple use cases including the Gaming environment and hand healthcare (e.g., Rheumatoid Arthritis (RA) monitoring).

This paper is organized as follows. Section 2 describes the glove hardware. Section 3 addresses the system implementation, the calibration of the glove anddescribes the graphical user interface (GUI). Section 4 describes the Data analytics and Post processing while Section 5 gives an account of the tests and results. Section 6 goes into the conclusions. The acknowledgment section closes the paper.

1.1. Virtual Reality (VR)

To be compatible with the Virtual Reality use case, it is important that any glove system developed for HCI adheres to the requirements detailed below:

Accuracy & Precision. Accuracy is the degree of closeness to a quantity's actual true value. Precision is the degree to which repeated measurements give the same quantity. Here, we define accuracy and precision to consist of position and orientation. Different parts of the hand should have priority for accuracy: a) Mapping of the center of the virtual hand is most important for many VR applications, b) The finger tips are next most important for accuracy as these joints can be estimated via inverse kinematics and other constraints, c) The skeleton/joints of the hand are next most important for accuracy.

Consistent recognition of gestures. Like speech recognition, if a gesture recognition system occasionally misinterprets signals then a break in presence occurs and users can become frustrated. Accidental gestures (known as false positives) are also a problem (e.g., accidentally signaling a command when unconsciously "talking with the hands").

Low latency. The faster the response of the system, then the more pleasant the user experience and the more easily users can enter a state of flow.

Simulation of button presses. Some applications will greatly benefit from simulation of button presses that provide a sense of self-haptic feedback (e.g., by touching two fingers together) and to control the game and system.

1.2. Rheumatoid Arthritis Assessment

RA is an auto-immune disease which attacks the synovial tissue lubricating skeletal joints and is characterized by pain, swelling, stiffness and deformity. This systemic condition affects the musculoskeletal system including bones, joints, muscles and tendons that contribute to loss of function and Range of Motion (ROM). Early identification of RA is important to initiate treatment, reduce disease activity, restrict its progression and ultimately lead to its remission. Clinical manifestations of RA can be confused with similar unrelated musculo-skeletal and muscular disorders. Identifying its tell-tale symptoms for early diagnosis has been the long-term goal of clinicians and researchers. Classifiers such as the Disease Activity Score (DAS) and Health Assessment Questionnaire (HAQ) provide an outcome measurement that reflects a patient's severity of RA disease activity. Such measurements are subjective and can be influenced by other factors such as depression or unrelated non-inflammatory conditions. Traditional objective measurement of RA using the universal goniometer (UG) and visual examination of the hands is labour intensive, open to inter rater and intra-rater reliability problems.

The DAS and HAQ [2, 3] are commonly used to measure disease onset and to assess disease status during clinical assessment [1]. Joint Stiffness is a common condition of RA that affects a patients' ability to perform basic activities and daily functions [4, 5]. Several objective measurement systems have been devised by researchers and assessed in clinical trials for effectiveness as a joint stiffness measurement device [6–11].

2. Tyndall Glove HW Description

The objective of our IMU Smart Glove is to quantitatively measure finger joint ROM including flexion, extension, adduction and abduction of the MCP, PIP and DIP joints of the fingers and thumb in degrees, together with thumb-index web space, palmar abduction to assist medical clinicians with the accurate measurement of the common condition of loss of movement in the human hand in patients with arthritis. All Smart Glove functionality is maintained,

controlled and analyzed by our in-house developed software system.

The described glove is a second generation iteration of the system by the authors as described in previous work [20].

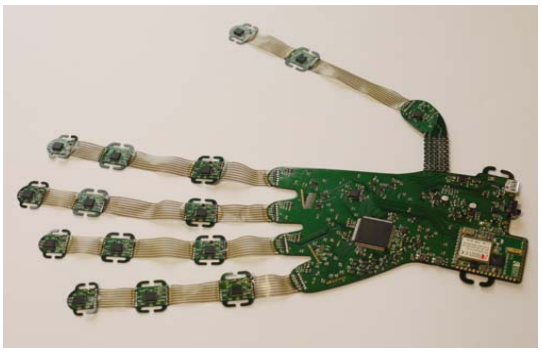

Fig. 1. The IMU Smart Glove rev 2.

2.1. System HW Description

The IMU glove, shown in Fig. 1, has been manufactured using a mix of stretchable & flexible technology. Stretchable areas of the device cross each finger joint so they can conform to the human hand.

The glove includes 16 9-axes IMU's (each including 3-axis accelerometer, 3-axis gyroscope and 3-axis magnetometer) strategically placed to account for the degrees of freedom (DOF) of each finger joint of the hand. IMUs are positioned on the stretchable interconnect and are located on the phalange of each finger segment to measure orientation and biomechanical parameters.

Each IMU provides 6 DOF motion information (3 translational + 3 rotational) and 3D orientation information. By placing an IMU at both sides of each finger joint, (that is one per each finger bone and another one on the palm of the hand), the relative orientation of each IMU is calculated and used to generate angular and velocity movement throughout flexion and extension exercise of each finger joint and to calculate splaying of each finger.

2.2. Microcontroller

The processor selected for use in the system is an Atmel AVR32 UC3C 32 Bit Microcontroller. This is a high performance, low power 32-bit AVR microcontroller with built in single precision floating point unit. It was selected to enable complex embedded algorithms focused on motion analysis to be developed for real time low power consumption operation.

2.3. Wireless Communication

The RS9110-N-11-22 [21] module shown in Fig. 2 is an IEEE 802.11b/g/n WLAN device that directly provides a wireless interface to any equipment with a UART or SPI interface for data transfer. It integrates a MAC, baseband processor, RF transceiver with power amplifier, a frequency reference, and an antenna in hardware. It also provides all WLAN protocols and configuration functionality. A networking stack in embedded in the firmware to enable a fully self-contained 802.11n WLAN solution for a variety of applications.

The module incorporates a highly integrated 2.4 GHz transceiver and power amplifier with direct conversion architecture, and an integrated frequency reference antenna. The RS9110-N-11-22 comes with flexible frameworks to enable usage in various scenarios including high throughput networking applications.

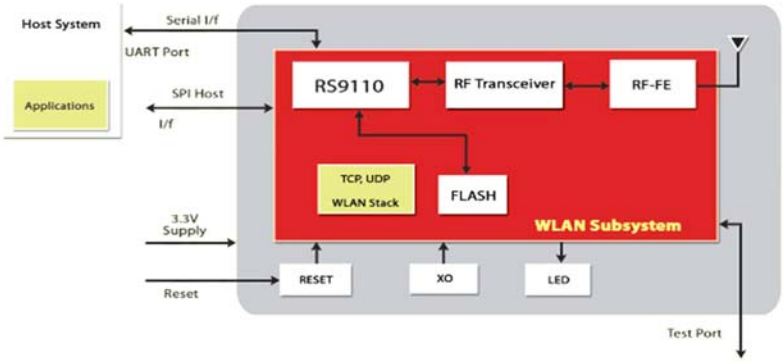

Fig. 2. RS9110-N-11-22 System Block Diagram.

The system operates according to a low complexity standard 4-wire SPI interface with the capability of operation up to a maximum clock speed of 25MHz. The communications module conforms to IEEE 802.11b/g/n standards and includes hardware accelerated implementation of WEP 64/128-bit and AES in infrastructure and ad-hoc modes. Themodule supports multiple security features such as WPA/WPA2-PSK, WEP, TKIP which makes it compatible with all medical ERP systems.

2.4. Sensors

The MPU-9150 [22] is a full three axis inertial measurement system incorporating tri-axis angular rate sensor (gyroscope) with sensitivity up to 131 LSBs/dps and a full-scale range of ±250, ±500, ±1000, and ±2000 dps, tri-axis accelerometer with a programmable full scale range of ±2 g, ±4 g, ±8 g and ±16 g and a tri-axis compass with a full scale range of ±1200 μT. This module incorporates embedded algorithms for run-time bias and compass calibration, so no user intervention is required. The MPU-9150 features three 16-bit analog-to-digital converters (ADCs) for digitizing gyroscope outputs, three 16-bit ADCs for digitizing accelerometer outputs, and three 13-bit ADCs for digitizing magnetometer outputs. For precision tracking of both fast and slow motions, the module features a user programmable gyroscope full-scale range of ±250, ±500, ±1000, and ±2000°/sec (dps), a user programmable accelerometer full-scale range of ±2 g, ±4 g, ±8 g, and ±16 g, and a magnetometer full-scale range of ±1200 μT.

2.5. Additional Features

To make the system adaptable in operation and compatible with a wide range of use cases outside the immediate application of RA monitoring, the IMU Smart Glove system also incorporates such features as optional storage via a micro SD card, battery monitoring and recharge facility, a USB bootloader, USB communication interface, and 15 Analogue inputs for optional resistive sensors (e.g., bend sensors or force sensors). The analogue front end is a buffered voltage divider to enable additional sensing functionality.

2.6. Flex Technology

The IMU Smart Glove PCB is a combination of flexible and stretchable PCB technology [33]. The stretchable material enables the microsystem to closely replicate mechanical properties of the human hand more accurately than standard flexible technology. As shown in Fig. 3, stretchable PCB sections are incorporated on hand areas crossing several finger joints to enable flexion at the knuckles and provide an interconnect mechanism between the "islands" of rigid PCB substrates which incorporate the WIMU technology.

The stretchable PCB technology is available from the company "Q.P.I. Group". The substrate material is polyurethane. it is possible to obtain a stretch factor of up to 30 % to enable wearable sensor system interconnect, depending on the design implemented on the copper pattern.

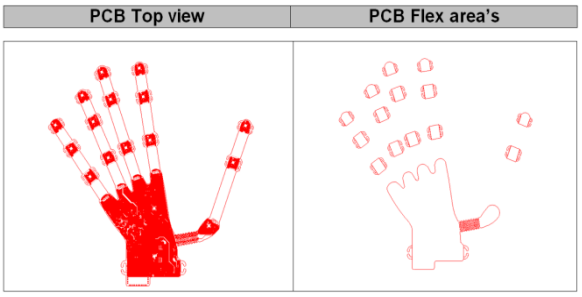

Fig. 3. PCB top view and flexible areas.

3. System Implementation

All the system embedded code is implemented using the Atmel Studio 6 IDE. Currently the implementation includes full application code that continuously reads sensor outputs and wirelessly transmits their data through a TCP socket.

The accuracy of IMU-based real time motion tracking algorithms is highly influenced by sensor sampling rate. Therefore a fundamental design requirement of the IMU Smart Glove was high application throughput to facilitate the development of algorithms using suitable PC SW such as MATLAB, C# and Unity. In addition, it was envisaged that once the algorithms would have been fully developed and tested, they would be fully implemented on the embedded platform. This eliminates the requirement for a high throughput device and allows for a low power implementation for example using BLE in a potential third generation of the glove.

To ensure maximum achievable sampling rates and computation time are compatible with the application scenario envisaged as specified in conjunction with clinical partners regarding signal temporal granularity, it was decided not to share the I2C bus between each of the 16 MPU9150's. Instead, dedicated I2C lines are provided to each one of the sensors and are driven in parallel. This provides the added advantage of ensuring synchronization between all IMU sensors.

3.1. Case 1. Raw Data Transmission

The embedded processor enables multiple modes of operation depending on the use case and degree of data granularity required. Having the wireless system transmitting raw data at the highest achievable data rate is desirable for the development of the analytics as it is more practical to develop them using PC based SW (real time or post processing) and then porting them to the embedded system than develop them directly within the embedded system.

3.2. Case 2. Transmission of Raw Data and Information

The wireless system transmits raw data and quaternions/rotation matrix (from gyros) at the highest

achievable data rate. Quaternions then will be subject to drift/errors and the analytics to correct for this are implemented within the controlling software. At this stage we have a clear idea of the maximum processing time that could be allocated in the embedding to this task and that is taken into consideration when designing these algorithms.

3.3. Case 3. Transmission of Processed Data

With the wireless system with full analytics embedded, the internal sampling rate of the sensors should be kept to a maximum achievable SR, the high wireless data rate might no longer be required.

The processing time (per sample cycle) allocated to the embedded tasks and estimated maximum sampling rate / Application Throughput with the microcontroller running at 48 MHz are shown in table I Depending on the computational complexity of the drift correction algorithm, (which are under development at the Tyndall Institute), different application data throughputs are achievable as shown in Table 1.

Table 1. Processing time requirements for motion data analysis.

	Raw data	**Raw Data + Quaternions**	**Full analytics embedded**
Sensor Sampling (16 IMUs)	~ 0.9 ms	~ 0.9 ms	~ 0.9 ms
Wireless Communications	~0.3 ms	0.4-0.5 ms	~0.4-0.5 ms
Quaternions / Rotation Matrix Algorithm	None	~ 0.3-0.5 ms	~0.3-0.5 ms
Drift correction algorithms	None	None	~ 8/3/2/1.33/0.5 ms
Estimated application throughput /data rate	~750 Hz / 2 Mbps	~500 Hz / 2 Mbps	100/200/250 /300/400 Hz

3.4. Calibration using Accelerometry and Gyroscope Datasets

Data glove accuracy and repeatability is affected by the non-linear nature of glove sensor output and any misalignment between the wearers hand and data glove sensor positioning. Data glove sensor calibration improves sensor accuracy and matches the boundaries of each sensor to those of each finger joint. A calibration routine requires the glove wearer to position groups of finger joints such as MCP's and PIP's at specific poses. Each pose places a finger joint group and relevant data glove sensors at their minimum and maximum boundaries. The IMU Smart Glove uses on-board sensors to automatically calibrate each glove sensor, regardless of the wearer's joint flexibility. Each glove accelerometer sensor is sampled when the hand is in a neutral position to calculate finger joint thickness and slope offset, and used during angular calculation. Accelerometers placed on each one of the finger's phalanges provide information with regards to the inclination to gravity of the phalanx. The output response of each sensor provides information on the orientation of the sensor to gravity as shown in Fig. 4. The orientation to gravity of each one of the sensors placed on adjacent phalanges can be used to estimate the flexion of the finger.

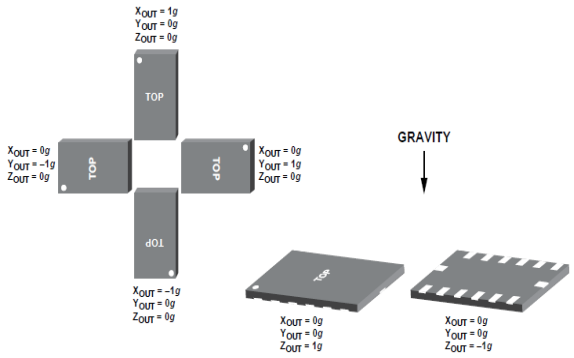

Fig. 4. Output response vs. Orientation to gravity

For example, if the measured acceleration for a specific finger from the medial phalanx accelerometer is (Xout, Yout, Zout) = (-1,0,0) g and from the proximal phalanx accelerometer is (Xout, Yout, Zout) = (0,0,1) g, it indicates a flexion of the PIP joint of 90 degrees. The inclination to gravity is determined according to the standard formulas (1), (2) and (3):

$$\theta = \tan^{-1}\left(\frac{A_{X,OUT}}{\sqrt{A_{Y,OUT}^2 + A_{Z,OUT}^2}}\right) \quad (1)$$

$$\psi = \tan^{-1}\left(\frac{A_{Y,OUT}}{\sqrt{A_{X,OUT}^2 + A_{Z,OUT}^2}}\right) \quad (2)$$

$$\phi = \tan^{-1}\left(\frac{\sqrt{A_{X,OUT}^2 + A_{Y,OUT}^2}}{A_{Z,OUT}}\right) \quad (3)$$

where θ is the angle between the horizon and the x-axis of the accelerometer, ψ is the angle between the horizon and the y-axis of the accelerometer, and φ is the angle between the gravity vector and the z-axis.

3.5. GUI/User Interface

Data is streamed in real-time according to the use cases outlined above and post processed by our controlling software. This software is called

'DigitEase' [34] shown in Fig. 5. A pivotal role of DigitEase is its ability to encapsulate movement associated with finger joints in real time. Fig. 5 shows an example of DigitEase's user interface.

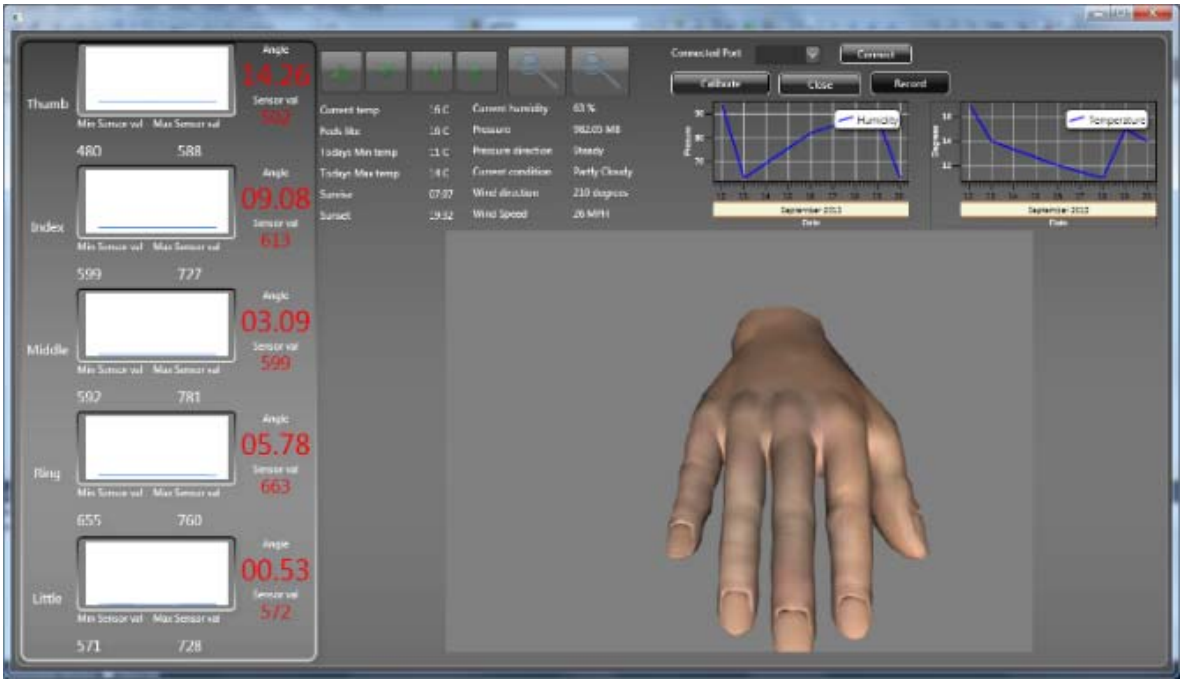

Fig. 5. Angular output from the data glove is displayed in 3D.

Algorithms segment recorded data to extract relevant flexion and extension movement information. Each piece of sensor data is categorised into pre-repetition, flexion, sustain, extension and post-repetition movement.

Fig. 6 demonstrates a typical flexion and extension angular movement profile used by DigitEase. Segmentation of finger joint movement is required to isolate flexion and extension movement data from unrequired pre-rep, port-rep and sustain time. Flexion and extension movement is analysed for initial and final angles. Both values represent minimum and maximum ROM information for movement repetitions and are indicators of completion and initialisation of flexion and extension movement.

DigitEase's data analysis dashboard presents post-segmented patient movement information. Fig. 7 shows an example of the dashboard.

The dashboard displays summary information on patient-completed exercise routines. It details individual repetitions and constituent sub-elements for each exercise routine. Colour coding of each repetition segment indicates performance information. Line charts graphically depict velocity, angle-angle and relative phase information for individually selected repetitions.

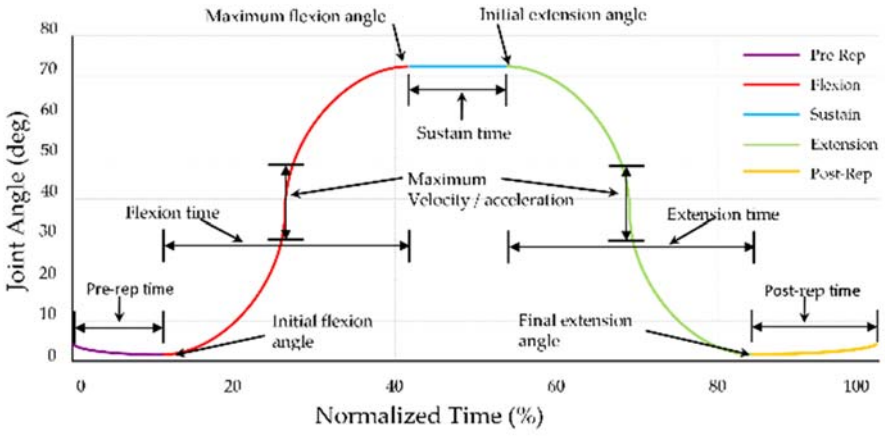

Fig. 6. Chart demonstrating segments that characterise segmentation of finger joint movement.

Fig. 7. DigitEase data analysis dashboard.

4. Data Analytics and Post Processing

Each angular calculation is low-pass filtered to remove sensor noise. A complementary filter with error control is implemented to combine accelerometer output with gyroscope rotation angle. Gyroscope rotational angle is initially accurate and drifts over time. Accelerometer angle cannot distinguish between lateral acceleration and rotation. The complementary filter acts as a high-pass and low-pass filter on both signals. It combines estimated gyroscope rotation and accelerometer angle to create an angular output.

4.1. Algorithms for Joint Angle Estimation

Fig. 8 shows the joints of the hand along with their number of degrees of freedom. The joint angles can be calculated as the result of the relative orientation of adjacent phalanges one to another so the algorithms to estimate the joints angles from the IMUs are based on the orientation estimation of the sensors themselves. This orientation is commonly represented by quaternions. Equations (4) - (7) represent the orientation / quaternions of adjacent phalanges that are linked by each joint.

$$\mathrm{q}_{\mathrm{palm,\,J}} = \mathrm{q}_{\mathrm{palm}} \tag{4}$$

$$q_{MCP,J} = {q_{palm}}^{-1} \times q_{MCP} \tag{5}$$

$$q_{PIP,J} = {q_{MCP}}^{-1} \times q_{PIP} \tag{6}$$

$$q_{DIP,J} = {q_{PIP}}^{-1} \times q_{DIP} \tag{7}$$

Over the years, a variety of algorithms for the estimation of orientation have been developed. The majority of these are quaternion-based algorithm and they can be divided in three main approaches: a) the *deterministic approach* (least-squares), b) the *frequency–based approach* (Complementary Filter) and c) the *stochastic* (Kalman filtering).

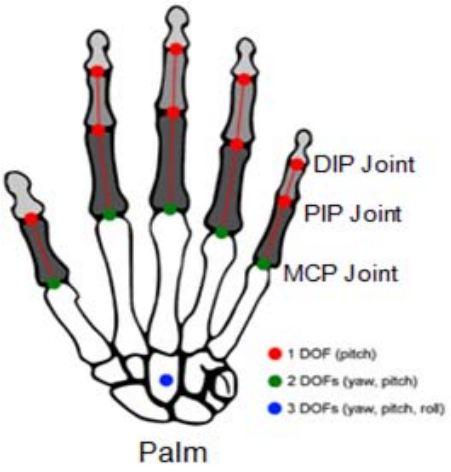

Fig. 8. Degrees of freedom of hand.

The *deterministic approach* was originally introduced in 1965, in the so-called Wahba's problem [30], which is a constrained least-squares optimization problem for finding the rotation matrix between two coordinate systems from a set of weighted vector measurements. Some of such algorithms are the TRIAD (Tri-axial Attitude Determination), QUEST (Quaternion ESTimator) and FQA (Factored Quaternion Algorithm). These algorithms are based on the concept of vector matching and require measurements of constant reference vectors.

The *frequency–based approach* fuses the orientation estimated from accelerometers and

magnetometers with the orientation estimated from gyroscope with a complementary filter. This filter blends the static low-frequency information provided by accelerometers and magnetometers, and the dynamic high frequency information provided by gyroscopes. The aim of the complementary filter is to ensure a compromise between the accuracy provided by short-term integration of the gyroscope data and the long-term measurements precision obtained by the accelerometer and magnetometer [31].

Stochastic estimation algorithms use a *dynamic model* for predicting aspects of the time behaviour of a system and a *measurement model* in order to produce the most accurate estimate possible of the system state. Among all stochastic algorithms, the Kalman filter is one of the most often used algorithms for tasks that involve multisensory fusion, filtering and motion prediction [32]. The filter works in a two-step process consisting of a prediction step and an update step. In the prediction step, Kalman filter produces estimates of the current state variables, along with their uncertainties. Once the outcome of the next measurement (corrupted with error and noise) is observed, these estimates are updated using a weighted average. Because of the algorithm's recursive nature, it can run in real time using only the present input measurement and the previously calculated state and its uncertainty matrix.

5. Testing Strategies and Results

Our new data glove was assessed for accuracy and repeatability and was compared with the 5DT state-of-the-art data glove. The Vicon MX motion capture system was used during accuracy testing to independently measure angular values generated at each finger joint. Movement was recorded by Vicon and simultaneously by DigitEase whilst each glove was placed on blocks of wood cut to specific angles. Angular readings were assessed using Root Mean Square Error (RMS) to provide an indicator of the variance between each estimated angular repetition value and the expected true value influenced by the angle on each block of wood. RMS error is influenced by both positive and negative errors which are either above or below the expected true value. Therefore RMS output is a measure of the angular error. Repeatability testing examined the ability of each data glove to consistently replicate angular readings when the subjects hand was held in a repeatable position. Testing strategies were originally developed to assess data glove suitability as a replacement for the UG. Although no formal set of repeatability testing strategies exist, the strategies used by [12] have been adopted by subsequent research groups [13, 16, 23–26] and are used in this study to allow comparison between study results.

The 'flat hand' test examines each data glove's ability to maintain a minimum repeatable value after full stretch of each data glove sensor. The plaster mould test examines the ability of each data glove to reproduce angular readings when positioned in a repeatable position. In all tests, our data glove was not calibrated for the subject, the 5DT data glove was calibrated.

5.1. 'Flat Hand' Results

The 'flat hand' test results demonstrated in Table 2 show that the IMU data glove outperformed the 5DT data glove. Mean MCP readings for the IMU glove were near-perfect -0.38°, with PIP readings of -2.53°. The 5DT produced readings of 4.17° for MCP and 2.27° for PIP. The results for our IMU glove are based on a system which is not calibrated before use.

Table 2. Comparison of mean angular readings recorded during 'flat hand' testing.

	5DT (Angle / SD)	**IMU (Angle / SD)**
Index MCP	2.34 (1.59)	-0.59 (1.87)
Index PIP	2.04 (1.05)	-2.74 (0.90)
Middle MCP	5.9 (0.55)	1.32 (2.26)
Middle PIP	3.27 (1.13)	-2.94 (1.25)
Ring MCP	5.14 (0.59)	-2.33 (1.21)
Ring PIP	1.02 (0.52)	-2.7 (1.11)
Little MCP	3.32 (0.88)	0.07 (2.56)
Little PIP	2.76 (1.32)	-1.75 (1.31)
Mean MCP	4.17 (0.90)	-0.38 (1.98)
Mean PIP	2.27 (1.0)	-2.53 (1.14)
Overall mean	3.22 (0.95)	-1.46 (1.56)

5.2. Plaster Mould Test Results

Table 3 shows comparison results for plaster mould testing for the 5DT and our IMU data glove. Readings showed the IMU Smart Glove produced better repeatability for MCP and PIP joints and better overall repeatability as indicated by the lower mean range angular reading. Comparison of mean range and SD readings from plaster mould testing for each data glove.

Table 3. Plaster mould test results.

Glove	**MCP**		**PIP**		**Mean**	
	Range	**SD**	**Range**	**SD**	**Range**	**SD**
5DT	8.85	2.13	6.23	2.09	7.54	2.11
IMU	5.99	1.89	5.10	1.58	5.55	1.74

5.3. Glove Finger Position Accuracy Results

Table 4 shows comparison of results for the 5DT and our IMU Smart Glove compared with the Vicon motion capture system and the UG.

Results showed the goniometer had greatest overall accuracy of 93.23 % with overall RMS of 2.76°. This is in agreement with typical findings on goniometric accuracy with 95 % of intratester reliability within 5° of measurement and intertester

reliability in the range of 7° to 9° [27–29]. The Vicon system provided mean accuracy of 89.33 % with RMS of 5.19°. Mean accuracy percentage for each sensor including mean error and overall accuracy percentage.

Table 4. Comparison between Tyndall WIMU Glove and 5DT Glove.

Sensor	Vicon	5DT	Goniometer	IMU
Index MCP	93.31	94.20	97.95	89.57
Index PIP	91.23	92.01	90.75	91.47
Middle MCP	91.46	79.66	95.83	82.40
Middle PIP	84.08	74.97	88.96	77.29
Ring MCP	87.20	70.46	97.37	82.02
Ring PIP	86.99	91.99	90.70	89.51
Little MCP	86.14	85.83	91.28	83.38
Little PIP	94.23	74.56	93.03	86.27
Overall accuracy %	89.33	82.96	93.23	85.24
RMS	5.19	7.15	2.76	5.95

This inaccuracy was most likely caused by noise, marker occlusion, and distance of reflective markers from Vicon cameras. Our IMU data glove provided best accuracy measurement of both data gloves and demonstrated similar accuracy to the Vicon measurement system. RMS results show that readings obtained from sensors contained approximately 5.95° of error. Results shown in Table 3 indicate that all sensors demonstrated accuracy between 82 % to 91 % except for the Middle PIP sensor that had accuracy of 77.29 %. This decreased accuracy may have been caused by slight stretch of sensor cable for this particular sensor.

5.4. Comparison with Previous Trials

The results shown in Table 5 compare 'flat hand' and plaster mould tests for the 5DT and our IMU data glove with previous research studies involving data gloves.

Table 5. Comparison of 'flat hand' and plaster mould tests with previous data glove studies.

Study	Flat hand test (Range / SD)	Plaster mould test (Range / SD)
Wise et al. [12]	4.4 (2.2)	6.5 (2.6)
Dipietro et al. [13]	3.84 (1.23)	7.47 (2.44)
Simone et al. [15]	1.49 (0.5)	5.22 (1.61)
Gentner and Classen [26]	2.61 (0.86)	6.09 (1.94)
5DT (this study)	2.27 (0.995)	7.54 (2.11)
IMU (this study)	4.86 (1.56)	1.74)

The 5DT data glove demonstrated range readings that out-performed data glove findings by [12] [13] and were similar to [26]. The data glove examined by [15] provided better results than all studies including the 5DT and our IMU glove. However this glove contained only 5 sensors that recorded movement of the MCP joints. The IMU glove performed better than all other data glove studies. Readings recorded by earlier studies are averaged for several subjects. This can hide higher inaccurate results for some subjects. For example, [12] recorded range readings from 5 subjects that varied between 2.5° to 6.7°. Results were averaged to 4.4°. Similarly, results from 'flat hand' testing from the study by [13] were summarised from a group of 6 male and female participants. Mean male range results went from 2.37° to 5.49° and mean female from 3.90° to 4.75°.

6. Conclusions

Data gloves have been proven to be a viable replacement for the UG and can offer unbiased finger joint ROM measurement. However their dependence on calibration reduces their usefulness in the many application spaces. The novel IMU based wireless Smart Glove detailed in this paper removes the requirement for sensor calibration using accelerometers and gyroscopes teamed with intelligent software techniques. Test results showed our IMU data glove had comparable repeatability to the UG with the added advantage of simultaneous angular measurement and removal of intra-tester and inter-tester reliability. Accuracy testing results showed the IMU data glove provided better accuracy and less overall error than the 5DT data glove with which it was compared. Of note the IMU glove required no calibration before use whilst maintaining results which demonstrated it had similar accuracy to the Vicon system.

Acknowledgements

The support of Science Foundation Ireland (SFI) as well as the National Access Program (NAP) support provided by the Tyndall National Institute is gratefully acknowledged. This work was also supported by Department of Education and Learning (DEL).

References

[1]. D. M. van der Heijde, van 't H. M, P. L. van Riel, and L. B. van de Putte, Development of a disease activity score based on judgment in clinical practice by rheumatologists, *J. Rheumatol.,* Vol. 20, No. 3, 1993, pp. 579–81.

[2]. J. F. Fries, P. Spitz, R. G. Kraines, and H. R. Holman, Measurement of patient outcome in arthritis, *Arthritis Rheum.,* Vol. 23, No. 2, 1980, pp. 137–145.

[3]. J. F. Fries, P. W. Spitz, and D. Y. Young, The dimensions of health outcomes: the health assessment questionnaire, disability and pain scales, *J. Rheumatol.,* Vol. 9, No. 5, 1982, p. 789-793.

[4]. P. Emery, F. C. Breedveld, M. Dougados, J. R. Kalden, M. H. Schiff, and J. S. Smolen, Early referral recommendation for newly diagnosed rheumatoid arthritis: evidence based development of a clinical guide, *Ann. Rheum. Dis.,* Vol. 61, No. 4, Apr. 2002, pp. 290–297.

[5]. F. C. Arnett, S. M. Edworthy, D. A. Bloch, D. J. McShane, J. F. Fries, et al., The American Rheumatism Association 1987 revised criteria for the classification of rheumatoid arthritis, *Arthritis and Rheumatism,* Vol. 31, No. 3, Mar-1988, pp. 315–324.

[6]. J. T. Scott, Morning stiffness in rheumatoid arthritis, *Ann. Rheum. Dis.,* Vol. 19, Dec. 1960, pp. 361–368.

[7]. V. Wright and R. J. Johns, Quantitative and qualitative analysis of joint stiffness in normal subjects and in patients with connective tissue diseases, *Ann. Rheum. Dis.,* Vol. 20, Mar. 1961, pp. 36–46.

[8]. M. L. Ingpen and P. H. Kendall, A simple apparatus for assessment of stiffness, *Ann. Phys. Med.,* Vol. 9, No. 5, Feb. 1968, pp. 203–205.

[9]. a Unsworth, P. Yung, and I. Haslock, Measurement of stiffness in the metacarpophalangeal joint: the arthrograph, *Clin. Phys. Physiol. Meas.,* Vol. 3, No. 4, Nov. 1982, pp. 273–81.

[10]. A. Howe, D. Thompson, and V. Wright, Reference values for metacarpophalangeal joint stiffness in normals, *Ann. Rheum. Dis.,* Vol. 44, No. 7, Jul. 1985, pp. 469–76.

[11]. E. Dionysian, J. M. Kabo, F. J. Dorey, and R. a Meals, Proximal interphalangeal joint stiffness: measurement and analysis, *J. Hand Surg. Am.,* Vol. 30, No. 3, May 2005, pp. 573–9.

[12]. S. Wise, W. Gardner, E. Sabelman, E. Valainis, Y. Wong, et al., Evaluation of a fiber optic glove for semi-automated goniometric measurements, *J. Rehabil. Res. Dev.,* Vol. 27, No. 4, 1990, p. 411.

[13]. L. Dipietro, A. M. Sabatini, and P. Dario, Evaluation of an instrumented glove for hand-movement acquisition, *J. Rehabil. Res. Dev.,* Vol. 40, No. 2, 2003, pp. 179–189.

[14]. L. K. Simone and D. G. Kamper, Design considerations for a wearable monitor to measure finger posture, *J. Neuroeng. Rehabil.,* Vol. 2, No. 1, Mar. 2005, p. 5.

[15]. L. K. Simone, N. Sundarrajan, X. Luo, Y. Jia, and D. G. Kamper, A low cost instrumented glove for extended monitoring and functional hand assessment, *J. Neurosci. Methods,* Vol. 160, No. 2, Mar. 2007, pp. 335–348.

[16]. G. Saggio, S. Bocchetti, C. A. Pinto, G. Orengo, and F. Giannini, A novel application method for wearable bend sensors, in *Proceedings of the 2nd International Symposium on Applied Sciences in Biomedical and Communication Technologies,* Bratislava, Slovakia, Nov-2009, pp. 1–3.

[17]. K. Li, I.-M. Chen, S. H. Yeo, and C. K. Lim, Development of finger-motion capturing device based on optical linear encoder, *J. Rehabil. Res. Dev.,* Vol. 48, No. 1, 2011, p. 69.

[18]. 5DT, 5DT Data Glove 14 Ultra, 2011. [Online], Available at: http://www.5dt.com/products/pdataglove14.html [retrieved: 01-2012].

[19]. Vicon Motion Systems, Vicon, 2013. [Online], Available at: http://www.vicon.com/. [retrieved: 01-2012].

[20]. B. O'Flynn, J. Sanchez, P. Angrove, J. Connolly, J. Condell, and K. Curran, Novel smart sensor glove for arthritis rehabiliation, in *Proceedings of the IEEE International Conference on Body Sensor Networks, (BSN 2013)*, May-2013, pp. 1–6.

[21]. Redpine Signals, RS9110-N-11-22: 802.11BGN wireless device server, RS9110-N-11-22 Product brief, 2008, [Online] Available at: http://www.redpinesignals.com/pdfs/RS9110-N-11-22 Wlan Module.pdf [retrieved: 01-2012].

[22]. MPU-9150 Product Specification Revision 4.0, *InvenSense*, California, Vol. 1, No. 408, 2012, pp. 1–52.

[23]. G. Kessler, N. Walker, and L. Hodges, Evaluation of the CyberGlove (TM) as a whole hand input device, GVU Technical Report, GIT-GVU-95-05, *Georgia Institute of Technology,* 1995.

[24]. M. Mentzel, F. Hofmann, T. Ebinger, B. Jatzold, L. Kinzl, and N. J. Wachter, Reproducibility of measuring the finger joint angle with a sensory glove, *Handchir Mikrochir Plast Chir,* Vol. 33, No. 1, 2001, pp. 9–64.

[25]. N. W. Williams, J. M. T. Penrose, C. M. Caddy, E. Barnes, D. R. Hose, and P. Harley, A goniometric glove for clinical hand assessment, *J Hand Surg Br.,* Vol. 25, No. 2, 2000, pp. 200–207.

[26]. R. Gentner and J. Classen, Development and evaluation of a low-cost sensor glove for assessment of human finger movements in neurophysiological settings, *J. Neurosci. Methods,* Vol. 178, No. 1, Mar. 2009, pp. 138–47.

[27]. A. Hellebrandt, E. Duvall, and M. Moore, The measurement of joint motion. Part III : Reliability of goniometry, *Phys Ther Rev,* Vol. 29, No. 6, 1949, pp. 302–307.

[28]. E. Lewis, L. Fors, and W. J. Tharion, Interrater and intrarater reliability of finger goniometrie measurements, *Am. J. Occup. Ther.,* Vol. 64, 2010, pp. 555–561.

[29]. N. B. Reese and W. D. Bandy, Measurement of Range of motion and muscle length: background, history and basic principles, Joint Range of Motion and Muscle Length testing, 2nd ed., *Saunders/Elsevier,* St. Louis, MO, 2010. pp. 3–29.

[30] G. Wahba, A least-square estimate of spacecraft attitude, *SIAM Rev.*, 8, 1965, p. 409.

[31] H. Fourati, N. Manamanni, Position Estimation Approach by Complementary Filter-aided IMU for Indoor Environment, in *Proceedings of the 12th biannual European Control Conference,* Zurich, Switzerland, July 2013.

[32] G. F. Welch, The use of the Kalman filter for human motion tracking in virtual reality, *Presence,* Vol 18, 2009.

[33] Brendan O'Flynn, J. T. Sanchez, James. Connolly, Joan. Condell, Kevin. Curran, Philip Gardiner, Barry Downes, Integrated Smart Glove for Hand Motion Monitoring, in *Proceedings of the 9th International Conference on Sensor Technologies and Applications (SENSORCOMM'15),* Venice, Italy, August 23 - 28, 2015, pp. 45-50.

[34] Connolly, J., Condell, J., Curran, K. and Gardiner, P., Towards Joint Stiffness measurement of Rheumatoid Arthritis sufferers, in *Proceedings of the 2nd European Conference on Design 4 Health (Design4Health),* Sheffield Hallam University, UK, SheffieldPub, 2013, pp. 150.